Development of a Software Model of a Heavy Vehicle Suspension for Research

Lloyd Davis[1], Dr. Jonathan Bunker[2]

Abstract
A Simulink Matlab control system of a heavy vehicle suspension has been developed. The aim of the exercise presented in this paper was to develop a Simulink Matlab control system of a heavy vehicle suspension. The objective facilitated by this outcome was the use of a working model of a heavy vehicle (HV) suspension that could be used for future research. A working computer model is easier and cheaper to re-configure than a HV axle group installed on a truck; it presents less risk should something go wrong and allows more scope for variation and sensitivity analysis before embarking on further "real-world" testing. Empirical data recorded as the input and output signals of a heavy vehicle (HV) suspension were used to develop the parameters for computer simulation of a linear time invariant system described by a second-order differential equation of the form:

$$f(t) = a\ddot{x} + b\dot{x} + cx$$

(i.e. a "2nd-order" system). Using the empirical data as an input to the computer model allowed validation of its output compared with the empirical data. The errors ranged from less than 1% to approximately 3% for any parameter, when comparing like-for-like inputs and outputs. The model is presented along with the results of the validation. This model will be used in future research in the QUT/Main Roads project Heavy vehicle suspensions – testing and analysis, particularly so for a theoretical model of a multi-axle HV suspension with varying values of dynamic load sharing. Allowance will need to be made for the errors noted when using the computer models in this future work.

Keywords: Heavy vehicle; suspension, computer modelling.

Introduction

The aim of the exercise presented in this paper was to develop a Simulink Matlab control system of a heavy vehicle suspension. The objective facilitated by this outcome was the future use of a working model of a heavy vehicle (HV) suspension that could be used for future research. A working computer model is easier and cheaper to re-configure than a HV axle group installed on a truck; it presents less risk should something go wrong and allows more scope for variation and sensitivity analysis before embarking on further "real-world" testing. Empirical data recorded as the input and output signals of a heavy vehicle suspension were used to develop the parameters for computer simulation of a 2nd-order system. Using the empirical data as an input to the computer model allowed comparison of the model output with empirical data. The model is presented along with the results of the validation. The programme to gather the data used three heavy vehicles. Only the school bus data and model will be treated in this paper.

Background

Heavy vehicle suspension parameters and definitions

Characterising heavy vehicle (HV) suspensions is central to the Australian VSB 11 test for “road friendliness” (Australia Department of Transport and Regional Services, 2004; European Council, 1996). Two measurements used to show that heavy

[1] PhD Student, School of Urban Development, Queensland University of Technology.
[2] School of Urban Development, Queensland University of Technology,

vehicle suspensions are road friendly are the damping ratio, zeta (ζ) and the damped free vibration frequency (f).

The damped free vibration (body-bounce) frequency is the frequency at which a truck's body has a tendency to bounce on its suspension with the largest excursions whilst the resultant motion is damped by the shock absorbers.

The damping ratio is a measure of how fast a system reduces its oscillations (and returns to quiescent or steady state) after a disturbance. It is a measure of the reduction in excursions of subsequent amplitudes of the output signal from a 2nd order system. In HV suspensions, it is related to a measure of how quickly the shock absorbers and other components reduce body bounce and wheel hop after the truck hits a bump. The damping ratio, zeta (ζ), is a dimensionless number and is usually presented as a value under 1.0 (e.g. 0.3) or a percentage (e.g. 30%) denoting the damping present in the system as a fraction of the critical damping value (Doebelin, 1980).

Parametric characterisation
Chesmond (1982) showed that system parameters may be characterised in a number of ways. Amongst these were:

- application of a random input signal to a system. Random signals are sometimes known as "white noise" and contain all frequencies in equal proportion. Fourier (or other frequency domain) analysis of the output signal resulting from that random input may be used to determine the characteristics of the system transfer function. The damped free vibration frequency (f) of the system characterises that transfer function and will show up as the largest magnitude peak in the frequency spectrum of the output signal after the application of "white noise" as an input signal; or

- application of an impulse input signal to a system: a perfect impulse signal contains all frequencies in equal proportion. Again, Fourier analysis of the output signal may be used to determine the characteristics of the system transfer function. Similar to random input signal excitation, the dominant (in this case, damped free vibration) frequency will manifest as the largest peak in the frequency spectrum of the output signal for a given impulse input.

Subjecting any system to an impulse signal and measuring the reducing excursions of the output signal enables the damping ratio of a system to be determined. The input signal used to excite the system is known as the forcing function. Doebelin, p79 (1980) showed by analysis, on the subject of length of time over which the impulse function is applied and its shape: 'We see that if [the input function's] duration is "short enough", the system responds in essentially the same way as it would to a perfect impulse of like area and that the shape of [the input function] makes no difference whatsoever.'

Damping ratio formulae – full wave
The damping ratio (ζ) may be determined by comparing the values of any two consecutive response peaks in the same phase (i.e. comparing the magnitudes of the 1st and 3rd excursions or the 2nd and 4th excursions) of the output signal of an

underdamped 2nd order system after an impulse function input has been applied (Meriam & Kraige, 1993). Prem, et al., (2001) used the formula (Meriam & Kraige, 1993):

$$\delta = \frac{2\pi\zeta}{\sqrt{1-\zeta^2}} \qquad 1$$

where:

δ is the standard logarithmic decrement (Meriam & Kraige, 1993) given by the following formula:

$$\delta = \ln\left(\frac{A_1}{A_2}\right) \qquad 2$$

as illustrated in Figure 1:

- A_1 is the amplitude of the first peak of the response; and
- A_2 is the amplitude of the third peak of the response,

to determine damping ratio.

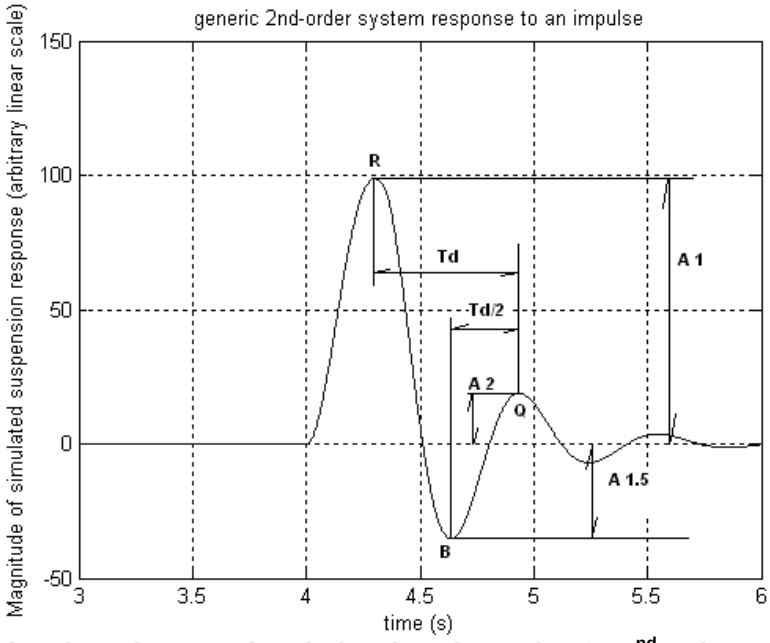

Figure 1: Illustrating the values used to derive damping ratio of a 2nd order system.

Alternatively, A_1 and A_2 may be described as the first two peaks of the response that are in the same direction (i.e. on the same side of the x-axis of the time-series signal of the response).

Where it is desired to determine damping ratio from a signal with more than 2 peak values of the signal on the same side of the x-axis in a time series, Thomson & Dahleh (1998) provide:

$$\delta = \frac{1}{n}\ln\left(\frac{x_0}{x_n}\right) \quad (3)$$

to substitute into Eq 1:
where:

- x_n is the amplitude after n successive cycles have elapsed; and
- x_0 is the amplitude when n = 0; or

for the case where continuous successive peaks are present (Technical Committee ISO/TC 22, 2000):

$$\delta = \ln\left[\frac{1}{n-1}\left(\frac{x_1}{x_2}+\frac{x_2}{x_3}+.....+\frac{x_n}{x_{n+1}}\right)\right] \quad (4)$$

Note: solving for ζ using Eq 1 results in the in the following equation (Meriam & Kraige, 1993) as shown in other work (Davis & Bunker, 2007):

$$\zeta = \delta \Big/ \sqrt{[(2\pi)^2 + \delta^2]} \quad (5)$$

Damping ratio formulae – half wave
Where a half-cycle of a 2nd- order system is present, the damping ratio may be derived from Eq 1, but using, as illustrated in Figure 1:

- the values of the first two peaks: A_1, $A_{1.5}$; and
- half the damped natural period $\frac{\tau_d}{2}$.

The period between A_1 and $A_{1.5}$ may be taken as half the damped natural period or $\frac{\tau_d}{2}$. From the same equations of motion used to derive Eq 1, by restating Eq 1 in all its terms, (Thomson & Dahleh, 1998):

$$\delta = \zeta\varpi_n \; \tau_d = \frac{2\pi\zeta}{\sqrt{1-\zeta^2}} \quad (6)$$

then, substituting $\frac{\tau_d}{2}$ for the period and adjusting the other sides of the equation for equality:

$$\delta_{1/2} = \zeta\varpi_n \frac{\tau_d}{2} = \frac{\pi\zeta}{\sqrt{1-\zeta^2}} \quad (7)$$

where:

- ζ = damping ratio;
- $\delta_{1/2} = \ln\left(\frac{A_1}{A_{1.5}}\right)$;
- ω_n = undamped natural frequency; and
- τ_d = damped natural period.

Now, equating only the first and last parts of Eq 6 yields:

$$\delta_{1/2} = \frac{\pi\zeta}{\sqrt{1-\zeta^2}} \qquad 8$$

$$\Rightarrow \quad \delta_{1/2}{}^2 = \frac{\pi^2\zeta^2}{1-\zeta^2}$$

$$\Rightarrow \quad (1-\zeta^2)\delta_{1/2}{}^2 = \pi^2\zeta^2$$

$$\Rightarrow \quad \zeta^2 = \frac{\delta_{1/2}{}^2}{\delta_{1/2}{}^2 + \pi^2}$$

$$\Rightarrow \quad \zeta = \sqrt{\frac{\delta_{1/2}{}^2}{\delta_{1/2}{}^2 + \pi^2}}$$

$$\Rightarrow \quad \zeta = \delta_{1/2} \Big/ \sqrt{\delta_{1/2}{}^2 + \pi^2} \qquad 9$$

n.b: this for $\delta_{1/2} = \ln\left(\frac{A_1}{A_{1.5}}\right)$.

We will need these equations for the analysis and derivation of the computer model later.

Experimental procedure

Test vehicle

The experimental procedure has been documented extensively elsewhere (Davis & Bunker, 2008). The following section provides a summary of the procedures and instrumentation used for the testing on the bus; the results of which are presented and analysed later in this paper. A school bus with two axles, one front and one rear (Figure 2), was used as the subject of this paper. It had standard manufacturers' suspension and was fitted new shock absorbers. This latter point to ensure that the suspension characteristics were as close as we could get to manufacturer's specification.

Figure 2: 2-axle school bus used for testing.

Instrumentation

The drive axle of the bus was instrumented. This consisted of accelerometers and air pressure transducers (APTs). Accelerometers (one per hub), were mounted at each hub of the bus drive axle. This was to measure vertical acceleration of the axle at its hubs.

Figure 3 shows the accelerometer mounting brackets glued to the drive axle of the bus.

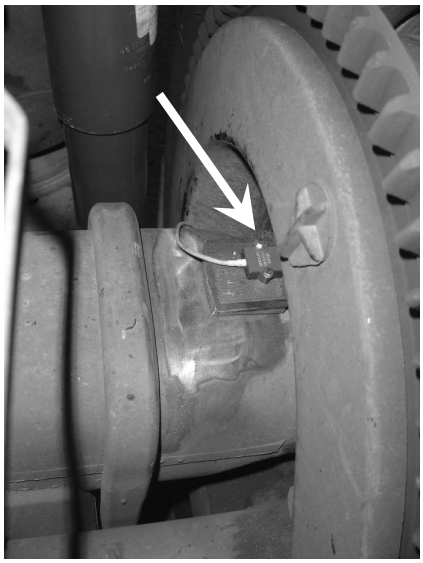

Figure 3: Accelerometer (arrowed) mounted on top of school bus axle.

Air pressure transducers (APTs) were mounted in the lines supplying air to the air springs as shown (arrow) in Figure 4. They measured air pressure in each air spring of interest and therefore the static and dynamic force between the spring and the chassis at that axle-end.

An advanced version of the TRAMANCO P/L on-board CHEK-WAY® telemetry system was used to measure and record the dynamic signals from the outputs of the APTs and accelerometers. The CHEK-WAY® system is subject to Australian Patent number 200426997 and numerous international application numbers and patents, which vary by country. The low pass filter cut-off frequency of the telemetry system

was set well above the frequencies of the signals in the range of interest (i.e. above 100 Hz). The telemetry system sampling rate was 1 kHz. Consequently, the recording and measurement instrumentation parametric limitations were well clear of any frequencies of interest. Further, any aliasing [3] would have occurred for frequencies above 500 Hz: frequencies that generally do not occur in HV suspensions and, were they present, were removed by the 100 Hz low-pass filtering.

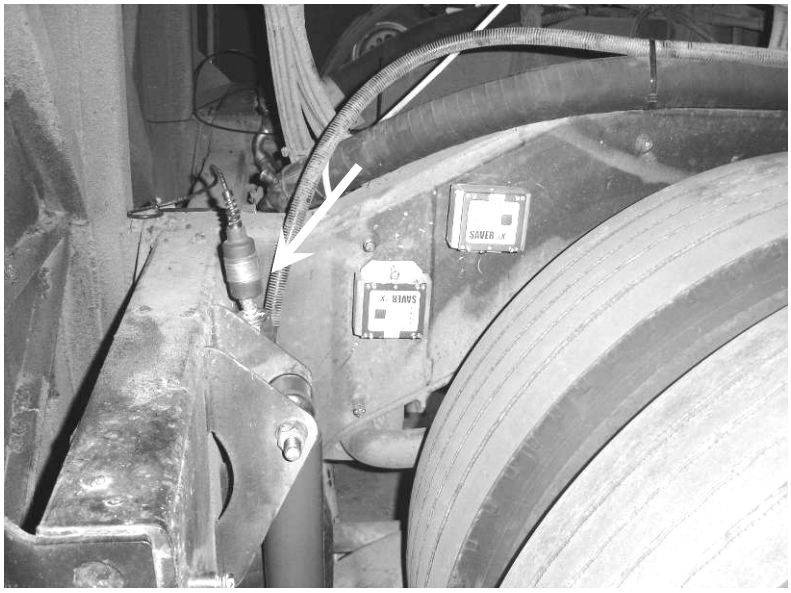

Figure 4: Air pressure transducer (arrowed).

Sampling frequency

The telemetry system sampling rate of 1 kHz meant that the sample interval was 1.0 ms. Note that the natural frequency of a typical heavy vehicle axle is 10 - 15 Hz (Cebon, 1999) compared with a relatively low 2 - 3 Hz for sprung mass frequency (de Pont, 1999). Any attempt to measure higher frequencies than body-bounce (such as axle-hop) using time-based recording would necessarily involve a greater sampling rate than when relatively lower frequencies (such as the body-bounce frequency) need to be determined (Houpis & Lamont, 1985). Since axle-hop was the highest frequency of interest for the analysis undertaken, the sampling frequency used by the telemetry system was more than adequate to capture the test signal data. This because its signal sample rate was much greater than twice any axle-hop frequency (e.g. 1 kHz sample rate vs. 15 Hz axle hop). In theory, a sampling rate of 30 Hz would have sufficed; industry practice would have suggested approximately 100 Hz, but a telemetry system with 1 kHz capability was available for the tests so was used. Accordingly, and to check the validity of the choice of sampling frequency, the Nyquist sampling criterion (Shannon's theorem) was met (Houpis & Lamont, 1985) with the issue of aliasing covered above.

VSB 11-style step test

The bus was loaded to maximum legal load and driven off an 80 mm step to replicate the VSB 11 step test (Australia Department of Transport and Regional Services, 2004). This procedure was repeated at least twice. The signals from the air pressure transducers on each air spring (Figure 4) and the accelerometers in Figure

[3] i.e. the tendency to fold signals with frequencies above half the sampling frequency back into the frequency range being measured (Davis & Bunker, 2007).

3 were recorded using the on-board telemetry system during this test procedure. Figure 5 to Figure 7 shows the detail of these tests for other vehicles in the programme, for example, but the bus was no different.

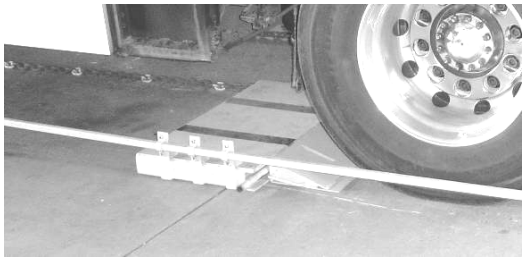

Figure 5: Before: showing preparation for the step test.

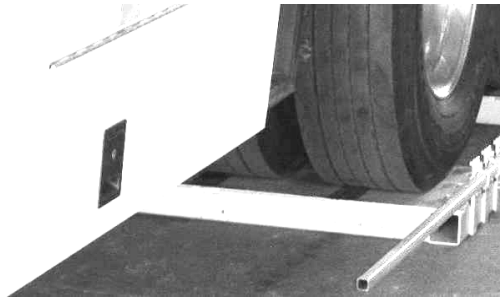

Figure 6: During: the rear axle ready for the step test.

Figure 7: After: the step test that was set up in Figure 5.

Figure 8: Close-up view of wheel rolling over the pipe during impulse testing.

Pipe test as an impulse

The bus was driven at, or just above, 5km/h over a 50 mm nominal diameter heavy wall pipe. The pipe had bars welded to it to prevent rotation as the tyres moved over it (Figure 8). The resulting impulse was thus applied to the suspension of the drive axle of the bus.

Results

General

The input and output signals recorded from the instrumentation mounted on the axles and air springs of the bus drive axle are shown in Figure 9 and Figure 10. These signals were used for system characterisation in the analysis section of this paper.

FFT processing of the accelerometer and APT signals was undertaken using the FFT function in MATLAB®. The raw data were not filtered before FFT processing. This allowed all frequencies present to be detected, processed from the time domain into the frequency domain and shown in the resultant FFT plots. The FFT plots of the accelerometer and APT signals have been included as Appendices. These show examples of the FFT plots of the LHS and the RHS accelerometer (input) signal and APT (output) signal from the bus drive axle recorded during the impulse testing outlined in the previous section.

The quiescent outputs of the instruments showed slight variations due to vehicle supply voltage fluctuations. These variations were not of great concern. Only the ratios of the signal excursions were important for determining damping ratio and zero-crossing periods for the frequency from the time domain. Hence left-right variations were either averaged out or the values from one side chosen (as an example, since the thrust here is “proof-of-concept”) as typical.

The figures in this section include the accelerometer data and the APT data for the axles of interest. Since there were two accelerometers and two APTs per axle, left and right hand side data are presented graphically in the one graph per axle per instrumentation type as:

- black trace: LHS; and
- grey trace: RHS.

Air spring data

The outputs of the APTs during the step test and the pipe test were recorded for each test vehicle. The signal magnitudes were proportional to the dynamic chassis-to-axle (body-bounce) forces within an experimental error previously determined at less than 1% (Davis, 2006c).

Figure 9 shows an example of a time series recorded from the bus drive axle APT signals during a VSB 11-style step test. Figure 10 shows an example of the same APT signals for a test where the HV was driven over the pipe as described above. In system analysis terms, the two time-series in Figure 9 and Figure 10 may be seen to be classical second-order impulse responses (Meriam & Kraige, 1993; Thomson & Dahleh, 1998).

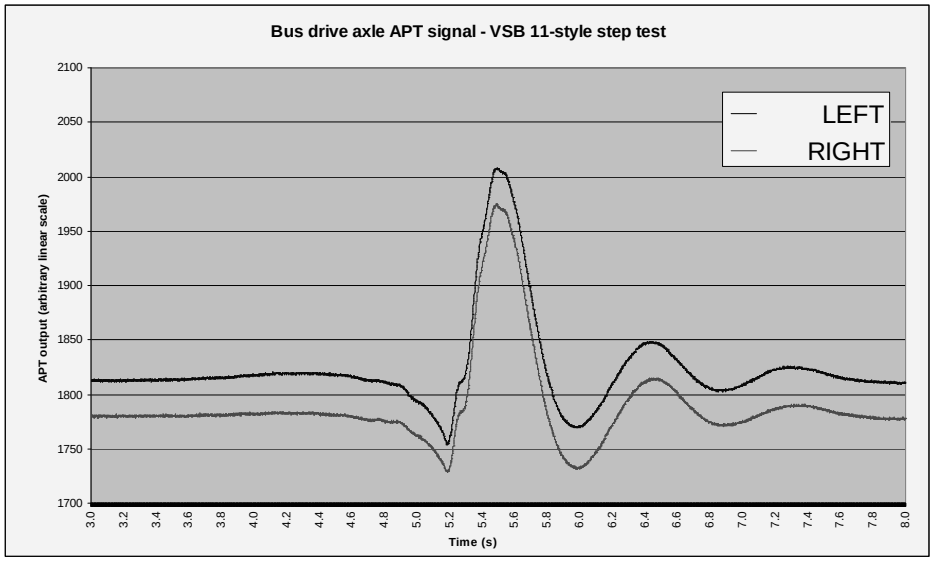

Figure 9: Time series of bus axle APT signals during impulse testing using VSB 11-style step test.

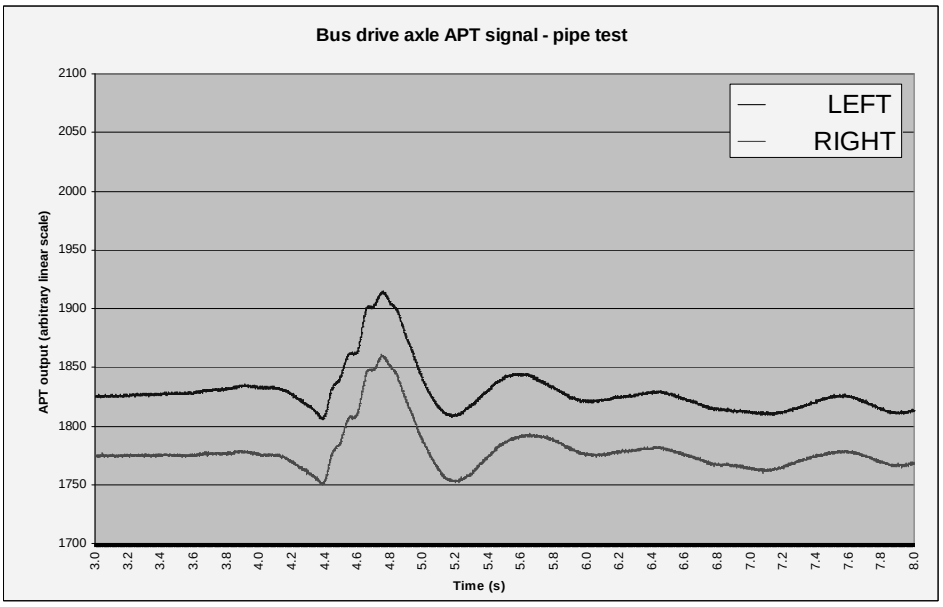

Figure 10: Time series of bus axle APT signals using pipe test as an impulse.

Accelerometer data

The acceleration at the ends of the drive axle was recorded from the outputs of accelerometers mounted at the hubs. This for the VSB 11-style step tests and the pipe tests. Figure 11 shows an example of a time series recorded at the bus drive axle from its accelerometers during a VSB 11-style step test; Figure 12 shows an example of the same accelerometer signals for the pipe test. Note that the excursions in Figure 11, particularly for positive-going data, are not exponentially reducing as for those in Figure 12. This was likely due to the difference in the two forcing functions with more body-bounce [4] from the VSB 11-style step test superimposed on the higher-frequency axle-hop. The analysis later used only body-

[4] compared with the pipe test.

bounce at the air springs so these differences in axle-hop excursions were not significant.

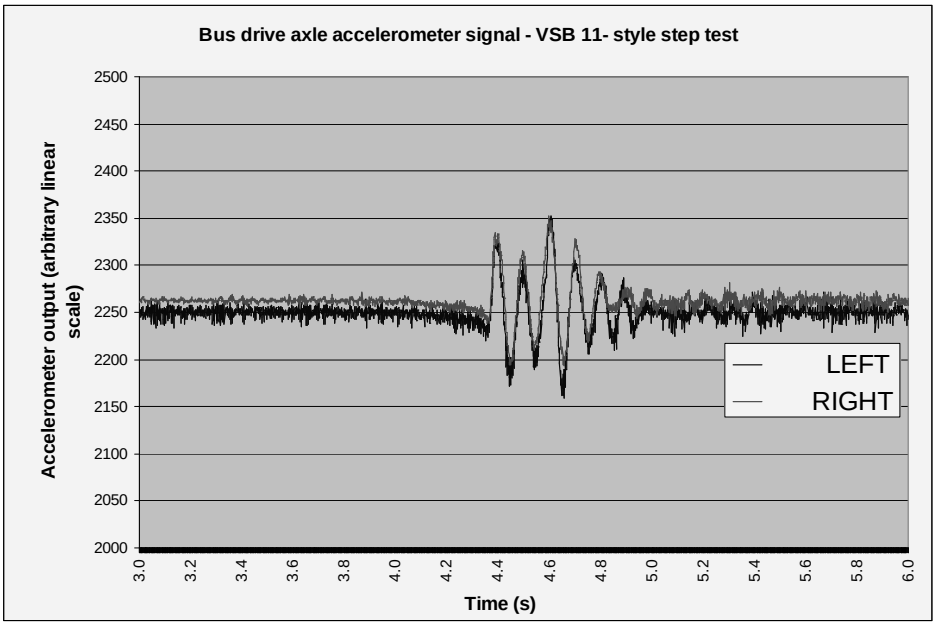

Figure 11: Time series of bus axle accelerometer signals during impulse testing using VSB 11-style step test.

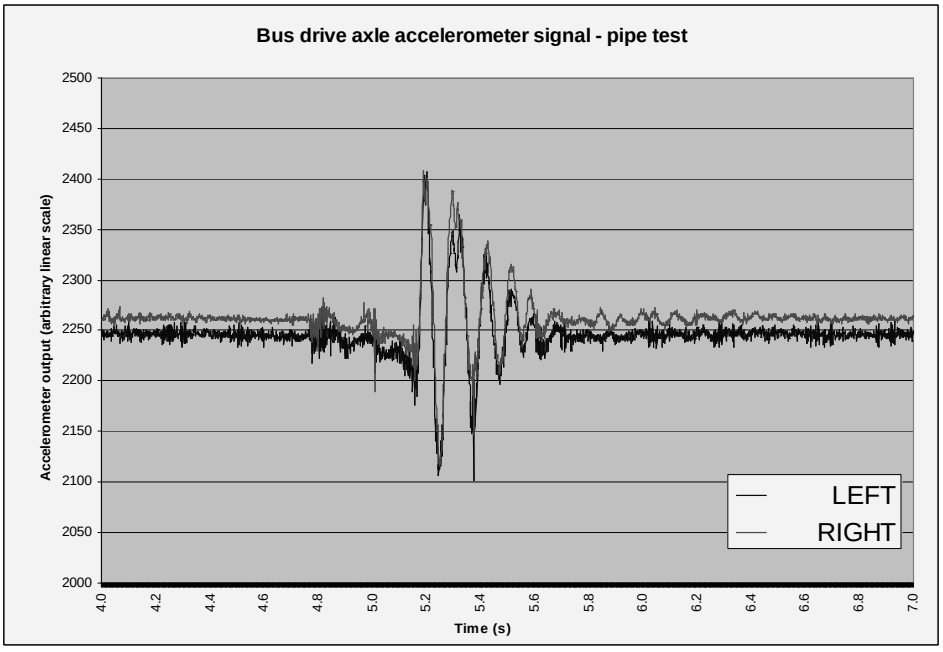

Figure 12: Time series of bus axle accelerometer signals using pipe test as an impulse.

Analysis

General

Damping ratios that were derived from empirical data measured during the VSB 11-style step tests and the pipe tests. Similarly, the damped natural frequency of the drive axle of the bus was derived from these two test methods. Further, the damping ratios and damped natural frequencies derived during the VSB 11-style step tests

and documented in this section are used later in this report for generating computer models of the test HVs' suspensions.

The damped natural frequency may be seen as a peak in the magnitude (y-axis) of the air-spring signal FFTs shown in Appendix 2; these are provided for information. An alternate method, simpler but just as effective as a FFT, is used below. It uses the time (period) between successive points on the waveform (e.g. successive peaks or successive zero-crossings) and take the inverse of that period to find the frequency. Figure 1 shows this time as *Td*.

From first principles:

$$f = \frac{1}{T_d};$$

10

hence inverting *Td* provides, for the cases following, the damped natural frequency. It is for noting that the SI derived unit for frequency or vibration is Hertz (Hz) of which the derivation is s^{-1}.

Damping ratio

Figure 9 provides a very good example of a classical model of an expected output response of an underdamped second-order system to an impulse function. Regarding Figure 9 and using the variables shown in Figure 1:

- it was fairly straightforward to derive the ζ for the single drive axle on the bus (Meriam & Kraige, 1993; Thomson & Dahleh, 1998);
- this is shown below; and
- it is not hard to see that the pipe test at low speed produced an output that replicated the classical model of response of an underdamped second-order system.

To derive ζ for the bus we can use the values for the variables A_1 and A_2 (as shown in Figure 1) from in Figure 9 and Figure 10 and substitute them into Eq 1. These are shown in Table 1.

Table 1: Comparison between damping ratios for the two types of impulse testing - bus

Variable	LHS		RHS	
	VSB 11-style step test	Pipe test	VSB 11-style step test	Pipe test
Quiescent signal value	1812	1824	1777	1774
A_1	180	78	178	75
A_2	34	16	34	16
ζ [from Eq 1 where $\delta = \ln\left(\frac{A_1}{A_2}\right)$]	0.2564	0.2342	0.2548	0.2388

A comparison between the derived LHS and RHS values for ζ then may be made for:

- the two types of impulse forcing function; and
- ζ using full cycle values for the variables A_1 and A_2.

Experimental error, including contributions from mechanical and manufacturing tolerances, was manifest as differences between the values of ζ for each excitation impulse method. Averaging each side for like test methods in Table 1 is shown in Table 2. Now comparing for the two different impulses as forcing functions, we note that:

- the ζ results derived from the responses measured from the APTs on the bus axle were similar;
- averaging the result within each method for both sides and comparing these resulted in a difference of -0.0191 across the two methods (an error of approximately -7.4%);
- the differences within the VSB 11-style step were 0.0016 (a variation of approximately 0.6%) in 0.24; and
- the differences within the pipe test were 0.0046 (or 1.96 %) in 0.25.

Accordingly, experimental error in ζ results for the two methods for the bus was small. Even so, this will need to be addressed and this issue is further explored in the Discussion.

Table 2: Comparison between L/R averaged damping ratios for the two types of impulse testing on the bus.

Variable	VSB 11-style step test	Pipe test
ζ averaged across LHS and RHS	0.2556	0.2365

Damped natural frequency

The damped natural frequency may be seen as a peak in the magnitude (y-axis) of the air-spring signal FFTs shown in the Appendix. Using the T_d^{-1} method discussed above (Equation **Error! Reference source not found.**), a 5 Hz filter was applied to the signals in Figure 9 and Figure 10 to smooth the waveform and thereby read *Td* off the plots. The resultant values for damped natural frequency are shown in Table 3.

Table 3: Comparison between derived damped natural frequencies for the two types of impulse testing: bus.

Variable	LHS		RHS	
	VSB 11-style step test	Pipe test	VSB 11-style step test	Pipe test
Damped natural frequency f (Hz)	1.07	1.17	1.05	1.17

Averaging each side for like test methods in Table 3 is shown in Table 4:

Table 4: Comparison between L/R averaged damped natural frequencies for the two types of impulse testing on the bus.

Variable	VSB 11-style step test	Pipe test
f averaged across LHS and RHS	1.06	1.17

Now comparing for the two different impulses as forcing functions, we note that the f derived for the drive axle of the bus from the two test methods had a difference of 10.4%. This was the error between the VSB 11-style step test as the reference method and the pipe test. This result was consistent with the order-of-magnitude of differences between methods in previous results (Davis, Kel, & Sack, 2007; Davis & Sack, 2004, 2006).

Accelerometer data

The accelerometer waveforms shown in Figure 11 and Figure 12 indicate that the impulse signal durations lasted approximately 0.4 - 0.6 s, regardless of impulse method. This length of time for the impulse input is used later in this paper to calibrate the computer models of the suspensions tested.

Using Equation **Error! Reference source not found.**), the axle-hop frequency for each test HV was found from the accelerometer data by inverting the accelerometers' period in Figure 11 and Figure 12. Indicative axle-hop frequencies were as shown in Table 5.

Table 5: Indicative axle-hop frequencies as measured at the accelerometer periods for the drive axle of the bus.

Test vehicle/axle	Axle-hop frequency (Hz)
Bus drive axle	8.5 – 10.2

The axle-hop frequencies were independent of excitation method. Note that these figures aligned well with the peaks in the magnitudes shown in the FFTs in Figure 21 to Figure 23.

Model of the suspension

General

A computer model of the bus suspension was developed. The known inputs and outputs were the accelerations at the axle and the air spring signals proportional to relative displacement between the axle and the chassis. The computer model was calibrated against the dynamic parameters derived from these data. The body-bounce signals from the VSB 11-style step tests were chosen as the reference case.

Now consider a diagram of a half-axle (*i.e.* the wheel in one corner of the bus, or the "quarter-bus") such as shown in Figure 13. The pressure in the air springs may be considered proportional to the displacement between the body and the axle, or a variable arising from the result of subtracting displacement x from displacement y.

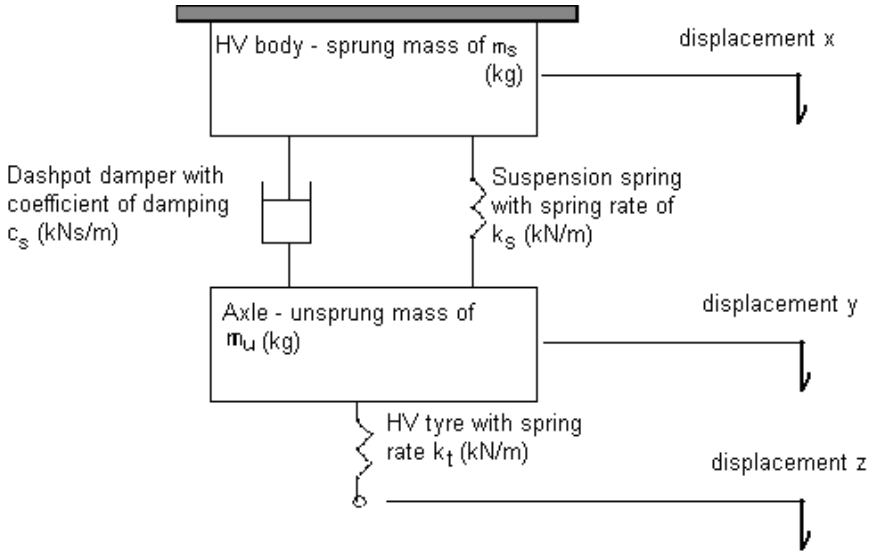

Figure 13: Diagram of a "quarter-axle" suspension of a HV showing parameters.

Since we knew the acceleration at the axles, this variable was used as the input signal to our model. Hence, the diagram in Figure 13 was reduced to that shown in Figure 14. This since the influence of axle mass was already present in the empirical acceleration signals measured at the axle.

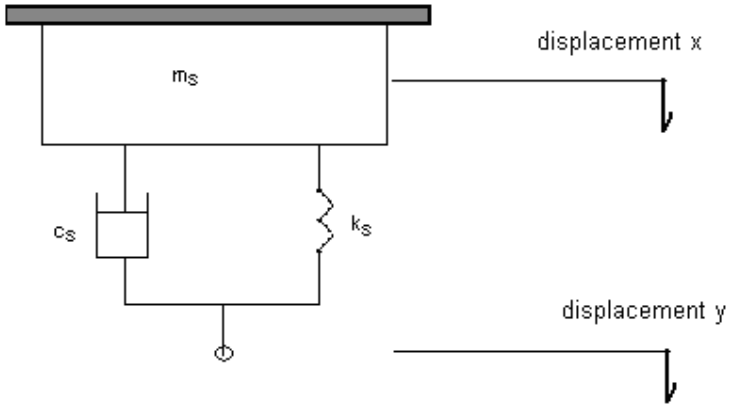

Figure 14: Simplified diagram of a "quarter-axle" suspension of a HV.

The responses at the air springs of the axle to the VSB 11-style step test impulses have been shown above. We assumed them classically underdamped second-order responses as indicated by the APT output waveforms from the VSB 11-style tests and the pipe test. We then constructed a simple computer model of the suspension conceptualised in Figure 13 and Figure 14 for the drive axle.

Assumptions

Non-linear HV spring rates over the entire range of spring travel have been included in computer models (Costanzi & Cebon, 2005, 2006). This extremely complex modelling also introduced some hysteresis (Costanzi & Cebon, 2005, 2006). However, Costanzi and Cebon (2005; 2006) noted that air spring hysteresis occurred over very small parts of the overall range. Other work (Cole & Cebon, 2007; Prem, George, & McLean, 1998) produced moderately-complex models of air-spring HVs that were used for research on pavement damage. Those models used a linear k_S value. Accordingly, for our simple model, we assumed a linear spring rate. Manufacturers' data (Mack-Volvo, 2007b) and the previous work on simple-to-moderately complex HV suspension models justified this assumption.

Similarly, even moderately-complex models of air-spring HVs used for research on pavement damage and suspension measurement have used models with a piece-wise linear damping coefficient, c, which varied depending on direction (Cole & Cebon, 2007; Duym, Stiens, & Reybrouck, 1997; Prem et al., 1998). Even the complex modelling of Costanzi and Cebon (2005; 2006) assumed linear, but unequal, damping coefficients in either direction.

Regarding the simple model in Figure 14, for purposes of deriving a computer model from the empirical data gathered during the testing and presented so far, some assumptions were therefore necessary:

- the spring rate, k_S, was linear regardless of direction;
- the damping coefficient, c_S, varied piecewise-linearly according to direction of movement (Costanzi & Cebon, 2005, 2006; Duym et al., 1997; Prem et al., 1998; Uffelmann & Walter, 1994);
- bushings, locating rods or other suspension components added no differential spring action, dead-band or hysteresis; and
- the springs and the dampers did not reach their limits of travel (*i.e.* no spring or damper hysteresis or position limiting).

System equations

The force on a damper is proportional to the relative velocities between its ends as defined by its damping coefficient c_s. The spring force is defined by its spring rate k_s and is proportional to the relative displacement between its two ends.

To derive the computer model, Newton's 2nd Law allows a system equation to be developed using these relationships. The relationship between x and y in Figure 14 was found by first summing the forces on m_s. To find these, the damper force and the spring force were included in Newton's 2nd Law as an equation:

$$\sum F = (m_s \ddot{x}) + c_s(\dot{x} - \dot{y}) + k_s(x - y) = 0$$

$$\Rightarrow \quad (m_s \ddot{x}) = c_s(\dot{y} - \dot{x}) + k_s(y - x) \qquad 11$$

where:

m_s = the mass of the system in kg;
c_s = the damping coefficient (*n.b. not* the damping ratio) of the shock absorber in kNs/m;
k_s = the spring constant in kN/m;
y = displacement of the axle in m;
$\dot{y}$ = velocity of the axle in m.s^{-1};
x = displacement of the body in m;
$\dot{x}$ = velocity of the body in m.s^{-1}; and
$\ddot{x}$ = acceleration of the body in m.s^{-2}.

Assuming underdamped behaviour, with some justification from the empirical evidence, the equations of motion from an underdamped 2nd-order system equation [remembering Eq 1)] provide:

the undamped natural frequency, $\omega_n = \dfrac{\omega_d}{\sqrt{1-\zeta^2}}$ 12

(ω_d will be simplified to ω from this point on)

where:

ω_d = the damped natural frequency or body-bounce frequency (Meriam & Kraige, 1993; Thomson & Dahleh, 1998) in radians.s^{-1}.

Second-order equation system model

Since the acceleration at the axle ($\ddot{y}$) was known from empirical data, it was used as an input to the model. However, it was not part of Eq 11 so needed to be integrated to find the velocity of the axle, $\dot{y}$, to implement the system equations in developing Eq 11 into a Simulink Matlab® control system block diagram in Figure 15:

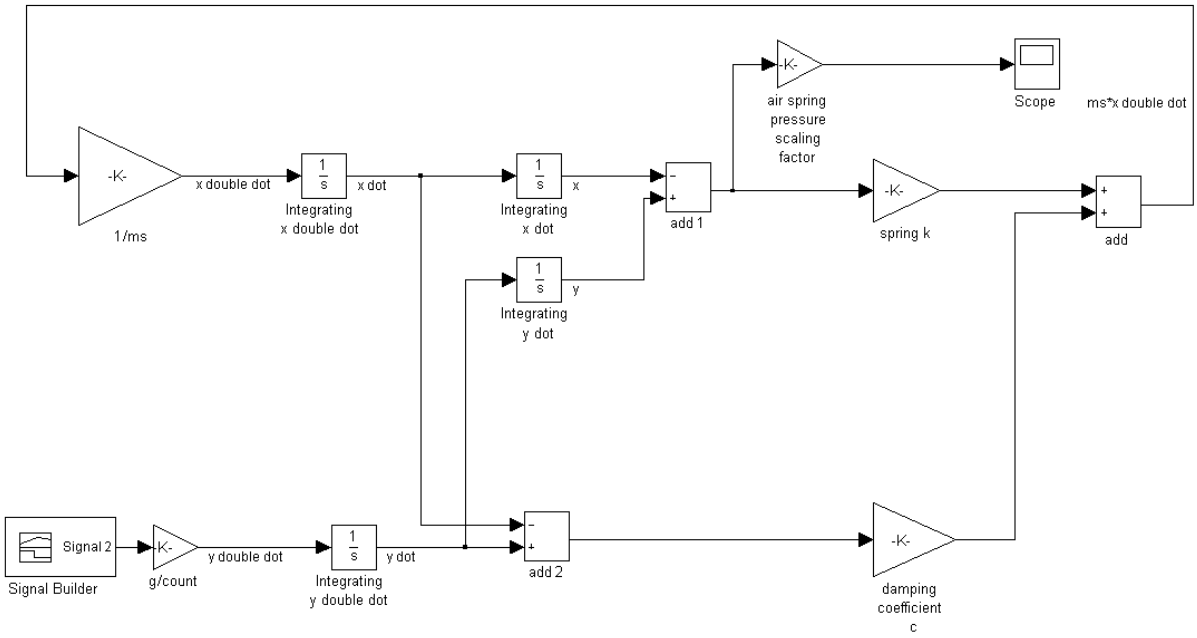

Figure 15: Matlab® Simulink block diagram using discrete block functions to execute the half-axle suspension system.

where:

- the output (Scope) was the APT pressure proportional to the displacement between the body and the axle (y - x); and
- the input signal (Signal 2) was $\ddot{y}$.

Mention needs to be made here of the non-linear characteristics of dampers with respect to direction, particularly directional velocity. The damping characteristic varies with direction of movement, more specifically, with the direction of velocity. This is to provide different dynamic resistances (i.e. damping coefficients) when the wheels hit a bump and then undergo rebound.

The different values of damping characteristic allow the suspension to control and optimise the tyres' contact with the road during travel over undulations and non-uniformities. This design feature required the determination of both bump and rebound damping ratios to derive the appropriate damping coefficients for each of the three vehicles. Accordingly, two damping coefficients were used in the computer models described in the following section: one for bump and one for rebound.

Influence of tyres

The impulse functions for these tests were measured from accelerometers at the axle, not the ground. Even so, tyre spring rate and tyre damping influenced the results of these tests. This because axle hop and tyre bounce were occurring and were components of the data recorded at the air springs and the accelerometers during the tests. Previous researchers have noted this effect (Fletcher, Prem, & Heywood, 2002). The FFTs in Figure 21 to Figure 23 show the axle-hop frequencies present at the hubs.

Table 6 shows some of the variables and their units which are contained in vehicle models incorporating tyre parameters.

Table 6: Parameters used in HV suspension models that include tyre characteristics.

Parameter	Symbol	Unit
Body-bounce frequency	ω	Radians.s^{-1}
Axle-hop frequency	ω_{axle}	Radians.s^{-1}
Damping ratio	ζ	n/a
Sprung mass	m_s	Kg
Unsprung mass m_u	m_u	Kg
Suspension spring rate	k_s	N/m
Suspension damping coefficient	c_s	Nm/s
Tyre spring rate	k_t	N/m
Tyre damping coefficient	c_t	Ns/m

The relationship between variables which constitute these vehicle models has been documented (Fletcher *et al.*, 2002). These are shown Eq 13 to Eq 15:

$$\omega = \sqrt{\frac{k_s k_t}{(k_s + k_t) m_s}} \qquad 13$$

$$\zeta = \frac{c_s}{2\sqrt{k_s m_s}} \left[\frac{k_t}{k_s + k_t} \right]^{1.5} \qquad 14$$

$$\omega_{axle} = \sqrt{\frac{k_s k_t}{m_u}} \qquad 15$$

Typical parameters for tyre spring rate and tyre damping coefficient have been reported (Costanzi & Cebon, 2005, 2006; de Pont, 1994; Karagania, 1997). These are shown in Table 7.

Table 7: Typical values used for tyre and HV suspension parameters.

Parameter	Symbol	Value
Tyre spring rate	k_t	1.96 MN/m
Tyre damping coefficient	c_t	1.76 kNs/m

Since the dynamic tyre phenomena undoubtedly influenced the data, we incorporated their influence by using Eq 13 to Eq 15 to derive c_s and k_s for our simplified models as follows. Manufacturer's data and previous research (Davis, 2006a, 2007, 2008; Davis & Bunker, 2008; Mack-Volvo, 2007a, 2007b; Prem, 2008) provided the unsprung and sprung masses. Since ω and ζ were derived for the test vehicle in the previous sections, Eq 13 was then rearranged to put known values on one side:

$$\Rightarrow \quad \omega = \sqrt{\frac{k_s k_t}{(k_s + k_t) m_s}}$$

$$\Rightarrow \quad \omega^2 = \frac{k_s k_t}{(k_s + k_t) m_s}$$

$$\Rightarrow \quad k_s m_s \omega^2 + k_t m_s \omega^2 = k_s k_t$$

$$\Rightarrow \quad k_s (k_t - m_s \omega^2) = k_t m_s \omega^2$$

$$\Rightarrow \quad k_s = \frac{k_t m_s \omega^2}{k_t - m_s \omega^2}$$

16

Hence a spring rate k (= k_s) and damping coefficient c_s the model in Figure 15 were able to be determined.

Similarly for Eq 14:

$$\Rightarrow \quad \zeta = \frac{c_s}{2\sqrt{k_s m_s}} \left[\frac{k_t}{k_s + k_t} \right]^{1.5}$$

$$\Rightarrow \quad c_s = \frac{2\zeta \sqrt{k_s m_s}}{\left[\frac{k_t}{k_s + k_t} \right]^{1.5}}$$

17

When we determined the spring rate k (= k_s) and substituted the value of ζ found in the previous sections, into Eq 17, the damping coefficient value for each suspension could be derived. Note that this process derived a value for k_s and c_s that incorporated a contributory component from the influence of the tyres on the empirical data.

As a check, Table 5 and the FFT plots in Appendix 2 provided the range of axle-hop frequencies. Once k_s and c_s were derived for the bus, the derived ω_{axle} value of 10.2 Hz (Table 8) was checked against the ω_{axle} values in Appendix 2 with good correlation.

Construction of a model

The impulse response at the bus air springs can be seen in Figure 9 and Figure 10. A computer model from the generalised diagram in Figure 15 was developed as follows and to populate the variables in Equation 11 as they applied to the bus in Figure 9 and Figure 10:

- the VSB 11-style step test provided an averaged ζ value of 0.256 (Table 2). Minor variation in derived ζ values between the two sides was compensated

for by averaging the LHS and RHS value of ζ of both sides listed in Table 1 (Table 2). These were, in turn, derived from the full-wave excursions in Figure 9 and the corresponding values shown for R and Q (Figure 1);

- the frequency was as shown in Table 4.

Since the pipe test was the test case and the reference method was VSB 11, the step test results for damped natural frequency from the latter were used. Again, variations in derived values between the two sides were allowed for by averaging the LHS and RHS values. This then resulted in a damped natural frequency, ω, for the model of 6.66 rad.s^{-1} (1.06 Hz). The undamped natural frequency ω_n, was found from Eq 12 by dividing by $\sqrt{1-\zeta^2}$:

$\omega_n = \omega / \sqrt{1-\zeta^2}$;

ω_n = 6.66 / $\sqrt{1-0.256^2}$; and therefore

ω_n = 6.89 rad.s-1 (1.097 Hz);

m_s = the sprung mass of the system.

A value of 4.47 t was derived from measured wheel mass of 5 t (Davis, 2006a, 2007, 2008) less the unsprung mass of the bus axle judged to be 530 kg (Prem, 2008).

Using known variables listed above in Table 7, Table 8 provides the remaining variables from Eq 16 and Eq 17.

Table 8: Given and derived tyre and HV suspension parameters - bus.

Parameter	Symbol	Value	Unit
Body-bounce frequency	ω	6.89	rad.s^{-1}
Sprung mass	m_s	4.47	t
Unsprung mass	m_u	0.53	t
Suspension spring rate	k_s	237.95	kN/m
Suspension damping coefficient	c_s	19.83	kNs/m
Tyre spring rate	k_t	1.96	MN/m
Axle-hop frequency	ω_{axle}	10.2	Hz

Manufacturer's data was provided for a static spring rate (k_s) range varying from 47.6 and 286.5 kN/m (Mack-Volvo, 2007a). Dynamic spring rates may vary by a multiple of up to 1.4 of static spring rates; typically about 1.33 (Costanzi & Cebon, 2005; Duym *et al.*, 1997; Prem *et al.*, 1998). This is explored later but suffice to say that this is due to the k_s value measured during static or quasi-static processes not accounting for adiabatic conditions (no heat transferred to the spring's surroundings) existing during short, transient excursions of the air spring. Note that the spring rate derived from empirical data was within the 47.6 to 286.5 kN/m range of the manufacturer's data (Mack-Volvo, 2007a).

As a check for axle-hop frequency derived here and shown in Table 8, the derived value had very good correlation to measured axle-hop frequencies in the range of 8.5 Hz to slightly greater than 10 Hz provided in Table 5 and Figure 21 to Figure 23.

The damping ratio for bump and rebound cases was determined from the signal excursions in the positive and negative directions from the VSB 11-style step tests, an example of which is shown in Figure 9. Figure 1 illustrates the starting points and conventions for derivation of differing damping ratios, depending on the relative direction of movement between the axle and the body. Referring to Figure 1:

- the convention for the signal excursion from R to B was taken as the case of rebound damping where the axle was moving away from the chassis;
- the signal excursion from B to Q was for the case of bump damping where the axle was moving toward the chassis.

The damping ratios were determined for the cases of:

- bump, where the body and axle were moving toward each other. This resulted in a positive sense for $\dot{y} - \dot{x}$ which, in turn, required the model to recognise only positive values of $\dot{y} - \dot{x}$ (i.e. a lower limit of zero for $\dot{y} - \dot{x}$): these were applied to the feedback loop as the bump damping coefficient; and;

- rebound, where the where the body and axle were moving away from each other. This resulted in negative values for $\dot{y} - \dot{x}$ which, in turn, required the model to consider only the negative values of $\dot{y} - \dot{x}$ (i.e. an upper limit of zero for $\dot{y} - \dot{x}$) to be applied as the rebound damping coefficient.

Accordingly, the values for A_1, $A_{1.5}$ and A_2 for the bus were used to derive ζ_{bump} and $\zeta_{rebound}$ using those excursions and Eq 9. These are shown in Table 10.

Having determined k_s and knowing k_t and m_s (Table 8), c_{bump} and $c_{rebound}$ were found by substituting the averaged LHS/RHS of the derived ζ_{bump} and $\zeta_{rebound}$ values (Table 2). The derived c_{bump} and $c_{rebound}$ values were as shown in Table 9.

Table 9: Determining the bump and rebound damping coefficients for the bus from the VSB 11-style step.

Parameter	c_{bump}	$c_{rebound}$
Formula	$\frac{2\zeta_{bump}\sqrt{k_s m_s}}{\left[\frac{k_t}{k_s + k_t}\right]^{1.5}}$	$\frac{2\zeta_{rebound}\sqrt{k_s m_s}}{\left[\frac{k_t}{k_s + k_t}\right]^{1.5}}$
Result	6.35 kNs/m	34.23 kNs/m

Table 10: Determining the bump and rebound damping ratios for the bus from the VSB 11-style step test.

Variable	LHS VSB 11-style step test	RHS VSB 11-style step test	average
Quiescent signal value	1812	1778	
A_1	169	164	
$A_{1.5}$	34	37	
A_2	27	28	
ζ_{bump} [from Eq 9 where $\delta_{1/2} = \ln\left(\frac{A_1}{A_{1.5}}\right)$]	0.071	0.093	0.082
$\zeta_{rebound}$ [from Eq 9 where $\delta_{1/2} = \ln\left(\frac{A_{1.5}}{A_2}\right)$]	0.457	0.427	0.442

This process yielded the values in Figure 16.

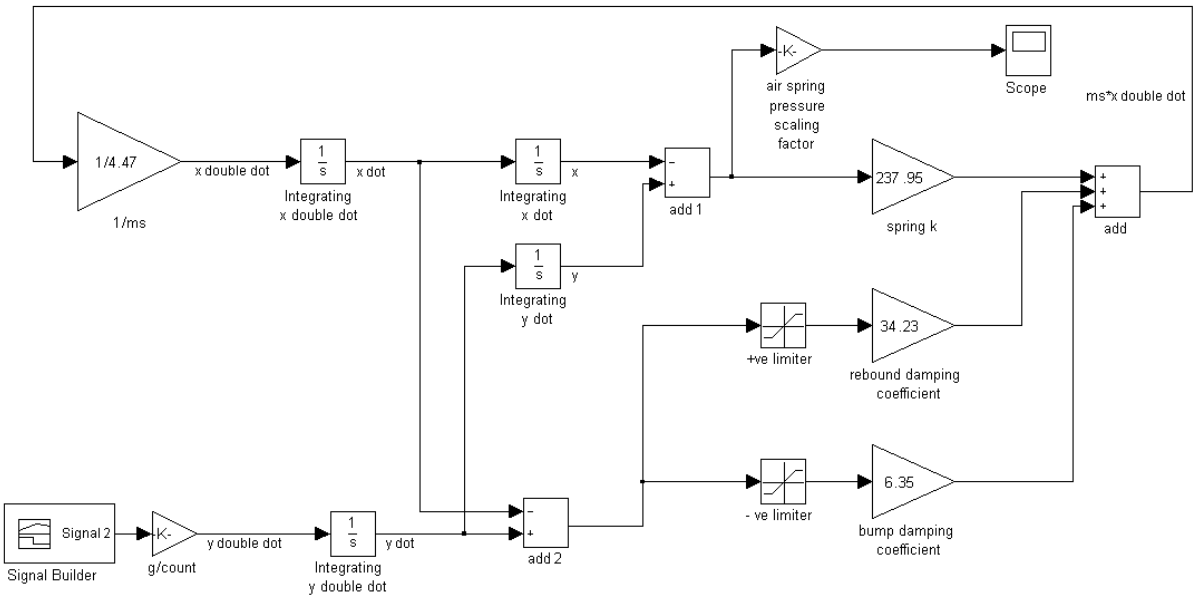

Figure 16: Matlab® block diagram showing individual blocks for bus half-axle suspension simulation.

Note that the manufacturer's data did not always match the characteristics derived here. This was particularly noticeable for the generalised damping coefficient, c, which was provided as an average value of 12.29 kNs/m for the H96 setting on this axle (Mack-Volvo, 2007a). Empirical extremes of c_{bump} at 3.2 kNs/m and $c_{rebound}$ of 30.3 kNs/m on this axle were also provided by the manufacturer (Mack-Volvo, 2007a).

The damping coefficient of a shock absorber will vary with velocity and direction. Nonetheless, the derived values of damper coefficients used here were justified since they were derived from empirically measured data (such as the excursions of the APT signals and the empirical damped natural frequency from the inverse of the time between excursions) and need to be viewed in light of variations due to manufacturing tolerances. Further, noting Eq 17, the spring constant k_s is proportional to the square of the natural frequency f. An empirically measured f will yield an empirical dynamic k_s. Finding k_s using dynamic data may result in a dynamic k_s value varying up to 1.4 times greater than static k (Costanzi & Cebon, 2005; Prem et al., 1998). In this case, the empirically-derived dynamic k_s value was within the manufacturer's data range.

The constants for the gain blocks before the output and after the input were determined from the relationship between the accelerometer signal values and the resultant APT output values with appropriate elimination of the steady-state signals on both due to gravity. This approach resulted in some non-alignment of the zero on the y-axes in the graphs following. The absolute values of the excursion maxima and minima from these models vs. those from the empirical data were not of great concern. This since damping measures were derived from the ratio of relative dynamic excursions in the y-axes data, not the offsets or absolute excursions.

Note that the positive sense of the pressure in the air springs was for relative movement of the axle and the chassis toward each other. The positive sense of $\dot{x}$ was for positive slopes of the air spring signal. Accordingly, $\dot{y} - \dot{x}$ was positive for the rising halves of the air spring signals (e.g. positive-going signals from B to Q in Figure 1) during the bump excursion, and $\dot{y} - \dot{x}$ was negative for the second halves of the air-spring signals (e.g. negative-going signals from R to B in Figure 1) during the rebound process. Further parametric investigation was then undertaken to derive simulation outputs for derived f and ζ values from the Simulink Matlab® model for the bus using:

- empirical data from the accelerometers during the VSB 11-style step test; and
- empirical data from the accelerometers during the pipe test.

The data from the accelerometers during the VSB 11-style step test was chosen as the reference value since this test is one of the tests defined and approved for use to type-test RFS in Australia. The duration of the impulse from the step test and the pipe test shown in Figure 11 and Figure 12 indicated that the duration of either impulse was approximately 0.4 s. This result validated, from the empirical data in this programme, previous theoretical work (Davis & Sack, 2006) which proposed that this duration was 0.43 s for the pipe test. Accordingly, for purposes of calibrating the model, an impulse signal from the accelerometers during the VSB 11-style step test was used.

Calibrating the model

Figure 11 shows an example of a VSB 11-style step test input signal measured at the axle using the accelerometers. It had a duration of approximately 0.4 s as explained above. Running the simulation for this empirical data from a representative sample from the accelerometers during the VSB 11-style step test input signal resulted in a

time-series output (from the "Scope" block in Figure 16) shown in Figure 17. This provided a combined average model of the LHS and RHS responses. Note that the plots within Figure 17 have been adjusted to align the x-axes for better comparison.

As a preliminary check, comparing the plots within Figure 17 visually with Figure 9, the period and excursions were very similar; a coarse validation that the model provided correlation with the empirical data. The values for f and ζ were then derived for the model's step test results in Figure 17. These are shown in Table 11 and Table 12 respectively.

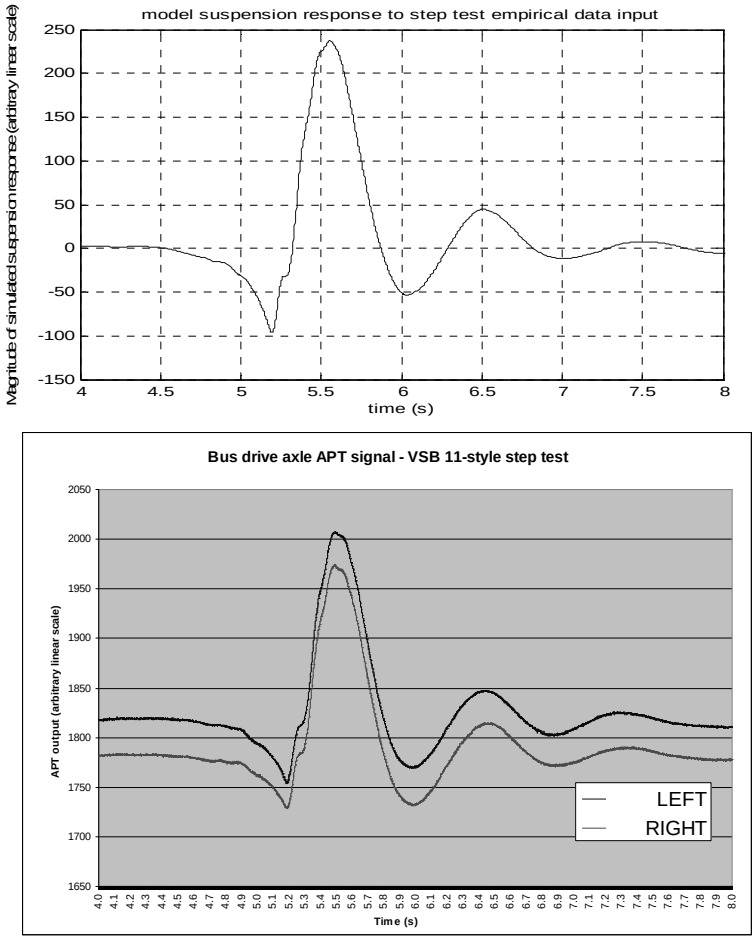

Figure 17: Time series of Matlab® Simulink bus half-axle model using VSB 11-style step test input signal from accelerometer (above) and Figure 9 (repeated below).

Empirical data as an input to the model – damping ratio

The computer model was provided with the empirical test input data measured from the accelerometers on the bus axle during the pipe test. The output signal from the simulated suspension model with empirical pipe test accelerometer data as an input is shown in Figure 18 with a reprised Figure 10 for comparison purposes.

The values for f and ζ were then derived from the model output trace in Figure 18. These are shown in Table 11 and Table 12 respectively in comparison to the f and ζ values from the step test data as an input to the model.

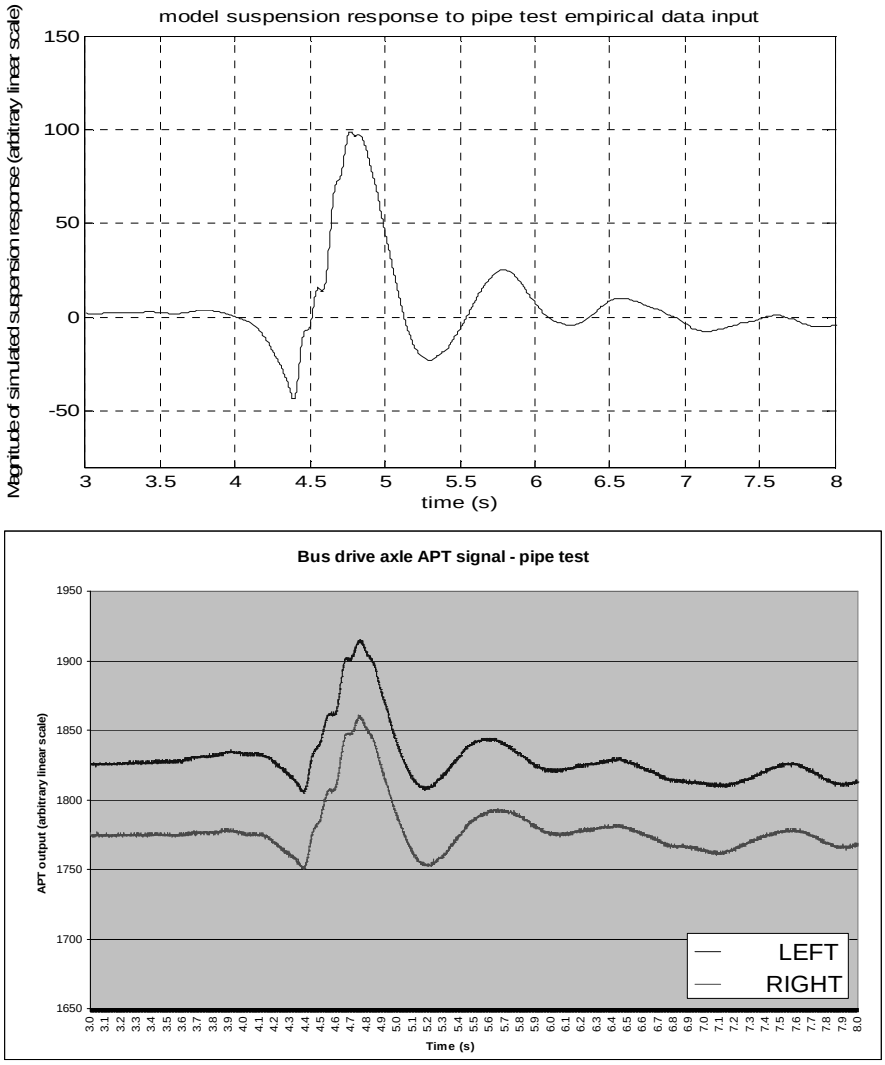

Figure 18. Time series of Matlab® Simulink model of the bus half-axle with empirical accelerometer data from pipe test as an input impulse (above) and Figure 10 (repeated below).

Table 11. Comparison between simulation model damping ratios and results from the two types of impulse testing.

Variable	VSB 11-style step test (average, both sides; Table 2)	Pipe test (average both sides; Table 2)	Simulink model with empirical input from VSB 11-style step test	Simulink model with empirical input from pipe test
Quiescent signal value			2.14	3.57
A_1			236.36	97.93
A_2			44.20	24.93
ζ [from Eq 5 where $\delta = \ln\left(\frac{A_1}{A_2}\right)$]	0.256	0.236	0.264	0.230
Error compared with average of actual VSB 11-style step test ζ (%)	0	-7.4	**3.2**	-11.1
Error compared with average of actual pipe test ζ (%)	8.1	0	11.6	**-2.8**

Table 11 shows a comparison between the derived ζ values from the bus model for the two inputs:

- empirical data from the accelerometers during the VSB 11-style step test (from Figure 11); and
- empirical data from the accelerometers during the pipe test, Figure 12.

In addition, Table 11 compares these to the results derived for ζ values from the two "live-drive" test methods, the variations between which have been covered above.

The differences in results from empirical data as inputs to the model were the same order-of-magnitude as noted in the results shown previously comparing the results from Table 2 with those in Table 11. The difference in the damping ratio for the empirical step test vs. the damping ratio for the step test from the model was 0.009 in 0.256 or an error of 3.5%. The difference between the model damping ratio from the pipe test compared with the empirical damping ratio was 0.006 (from Table 2) or an error of -2.8%. That is, the Simulink model provided results that differed, at worst, from the empirical data from the "live drive" test by 3.2%.

Empirical data as an input to the model – damped natural frequency

As discussed above, the output from the Simulink Matlab® model for the "quarter-bus" suspension model was measured for the following inputs:

- empirical data from the accelerometers during the VSB 11-style step test; and
- empirical data from the accelerometers during the pipe test.

Using the T_d^{-1} method discussed in the previous section, the damped natural frequency values for the two simulation inputs to the computer model of the bus were

derived from the model responses in Figure 17 and Figure 18. These are shown in Table 12 along with the averages of the measured values in Table 3 used to derive the computer model.

Table 12. Comparison between simulation model damped natural frequencies and results from the two types of impulse testing- bus.

Variable	VSB 11-style step test (average, both sides; Table 3)	Pipe test (average, both sides; Table 3)	Simulink model with empirical input from VSB 11-style step test	Simulink model with empirical input from pipe test
Damped natural frequency (Hz)	1.06	1.17	1.064	1.04
Error compared with average of actual VSB 11-style step test *f* (%)	0	9.40	**0.38**	-1.92
Error compared with average of actual pipe test *f* (%)	-10.38	0	-9.96	**-1.89**

The derived damped natural frequency from empirical data for the VSB 11-style step test (from which we took our model frequency) was 1.06 Hz. The errors between the simulated result *vs*. the pipe test and the simulated result *vs*. the VSB 11-style step test were -1.89 % and 0.38% for the respective inputs. This was less than the previous errors in empirical f results from manufacturer's certified VSB 11 values vs. f derived from the pipe test (Davis & Sack, 2004, 2006). Again, the Simulink model provided results that differed very little from the empirical data from the "live drive" test.

Given that the only variation in the two tests was the excitation method, the differences the empirical frequency outcomes of 1.17 Hz for the pipe test vs. 1.06 Hz for the step test must be attributed to the difference in excitation provided by them. It was therefore likely that the pipe test provided a higher f value because of the rise-then-fall nature of the impulse compared with the simple falling mechanism of the step down test. Further, the maximum time of pulse recommended by Doebelin (1980) for the impulse duration was 0.35**Td*. Both the step and pipe mechanisms' duration of 0.4 s was slightly longer than this recommendation and hence provided slightly longer impulse times than this the 0.35**Td* recommended by Doebelin (1980). This slight increase in duration probably made the difference in the measured values for damped natural frequency as shown in the analysis done by Doebelin, pp 79-81 (1980).

Error analysis

Table 13 provides a summary of the errors across all of the processes documented herein for:

- live-drive testing and analysis thereof; and
- analysis of computer simulation of empirical data.

Totalised errors across all testing and simulations – bus drive axle

Parameter	Method				
	Live drive **VSB 11 (left-right variation)**	**Live drive** **Pipe test compared with empirical VSB 11 result**	**Model** **VSB 11 input compared with empirical VSB 11 result**	**Model** **Pipe test input compared with empirical VSB 11 result**	**Model** **Pipe test input compared with empirical pipe test result**
ζ	0.6%	-7.4%	**3.2%**	-11.1%	**-2.8%**
f	1.9%	9.4%	**0.38%**	-1.92	**-1.89**

Table 13. Summary of errors across all methods - bus.

Conclusion

Prior experience (Davis & Sack, 2004, 2006) led to the conclusion, when formulating this test programme, that the pipe test results would yield an analysable, classical second-order result for the APT signals. This expectation was borne out. Accordingly, a computer model was developed. When actual data gathered from the accelerometers during VSB 11-style testing were used as inputs to the generalised computer model, the results correlated well to the actual data.

Given:

- the simplicity of the model;
- that the RHS and LHS f and ζ were averaged and therefore the models were composites derived, in part, from empirical data from both sides of the vehicles;
- the models excluded a number of mechanical suspension complexities; and
- that consideration needs to be made regarding that exclusion of a number of mechanical suspension complexities,

the results from the computer model for damped natural frequency and damping ratio gained from it in this paper compared very favourably with the empirical results. Now that the model's outputs have been validated against empirical data for f and ζ, the model and its derived parameters will be used for future work with further development. The errors ranged from less than 1% to approximately 10%, depending on parameter. When comparing like-for-like inputs and outputs, the errors reduced to just over 3%, at worst, for any parameter.

Given the sensitivity of derivation of damping ratio (ζ) to method (Uffelmann & Walter, 1994), this was a better-than expected result. A computer model has been derived from empirical data and validated against empirical data inputs with, again, an error of not more than approximately 10% at worst. This model will be used in future research in the QUT/Main Roads project Heavy vehicle suspensions – testing and

analysis, particularly so for a theoretical model of a multi-axle HV suspension with varying values of dynamic load sharing. Allowance will need to be made for the errors noted in this section when using the computer models in this future work.

That air-spring data supplying HV on-board mass systems may be used for characterisation of HV suspensions is a possibility that is being examined presently (Davis, Bunker, & Karl, 2008; Karl, 2007). One issue to be addressed in the future will be the sampling frequency of these systems as installed in HVs in service. Previous testing has used a Tramanco telemetry system with sample intervals of 24.0 ms (41.66 Hz) with good results (Davis, 2006b; Davis & Sack, 2004). That such sampling frequencies can be used with equivalent results to that from systems sampling at 1 kHz has been verified recently in other work (Germanchev & Eady, 2008).

Thank you

The authors would like to thank:

- Dr Hans Prem of MSDynamics for his advice on, and review of, the computer models;
- Dr Michael Mason of QUT for his assistance in reviewing the systems engineering sections in this report;
- the people at Tramanco for technical assistance in cutting up the axle/s, installing and removing the HV telemetry system and the transducers and test equipment;
- the people at Volvo (in various Australian States) for technical assistance and much patience rectifying the buses after we took the brakes apart to install the accelerometers;
- the Queensland Transport Darra depot transport inspectors who lent us their scales at a moment's notice;
- the RTA of NSW who contributed funding when we ended up with more test vehicles than our original budget allowed for;
- the people at Mylon Motorways for technical assistance, supply of drivers and the loan of the buses; and
- the people from Haire Truck and Bus for drivers for technical assistance.

Appendix 1 – Definitions, Abbreviations & Glossary

Terms, abbreviations and acronyms	Meaning
APT	Air pressure transducer. A device for emitting an electrical signal as a proportional surrogate of input air pressure.
Axle hop	Vertical displacement of the wheels (and axle), indicating dynamic behaviour of the axle and resulting in more or less tyre force onto the road. Usually manifests in the frequency range 10 – 15 Hz.
Body bounce	Movement of the sprung mass of a truck as measured between the axles and the chassis. Results in truck body dynamic forces being transmitted to the road via the axles & wheels. Usually manifests in the frequency range 1 – 4 Hz.
Damping ratio	How much the shock absorbers reduce suspension bounce after the truck hits a bump. The damping ratio, zeta (ζ) is given as a value under 1 (e.g. 0.3) or a percentage (e.g. 30%).
FFT	Fast Fourier transform. A method whereby the Fourier transform is found using discretisation and conversion into a frequency spectrum.
Fourier transform	A method whereby the relative magnitudes of the frequency components of a time-series signal are converted to, and displayed as, a frequency series. If the integrable function is h(t), then the Fourier transform is: $\phi(\omega) = \int_{-\infty}^{+\infty} h(t) e^{-i\omega t} dt$ Where: ϕ is the Fourier series; ω is the frequency in radians/s; and $i = \sqrt{-1}$ (Jacob & Dolcemascolo, 1998).
HV	Heavy vehicle.
Hz	Hertz. Unit of vibration denoting cycles per second or s-1.
NTC	National Transport Commission
RFS	"Road-friendly" suspension. A HV suspension conforming to certain limits of performance parameters defined by VSB 11. (Australia Department of Transport and Regional Services, 2004)
VSB 11	Vehicle Standards Bulletin 11. A document issued by DoTaRS that defines the performance parameters of "road-friendly" HV suspensions.

Appendix 2 – FFT plots

For purposes of comparison of the two forcing functions used to excite the suspensions via an impulse, viz: the pipe test and the VSB 11-style step test, the following Appendix shows examples of the FFTs from the bus drive axle air springs and accelerometers. This will allow comparison of the peak magnitude in the FFTs (and therefore the corresponding resonant damped frequency) between the two test methods.

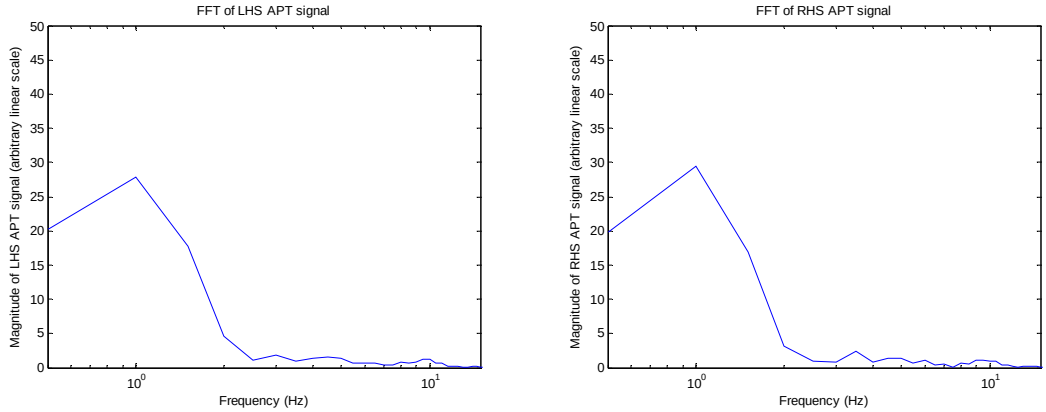

Figure 19: FFT of bus drive axle APTs – pipe test as impulse. Test 244

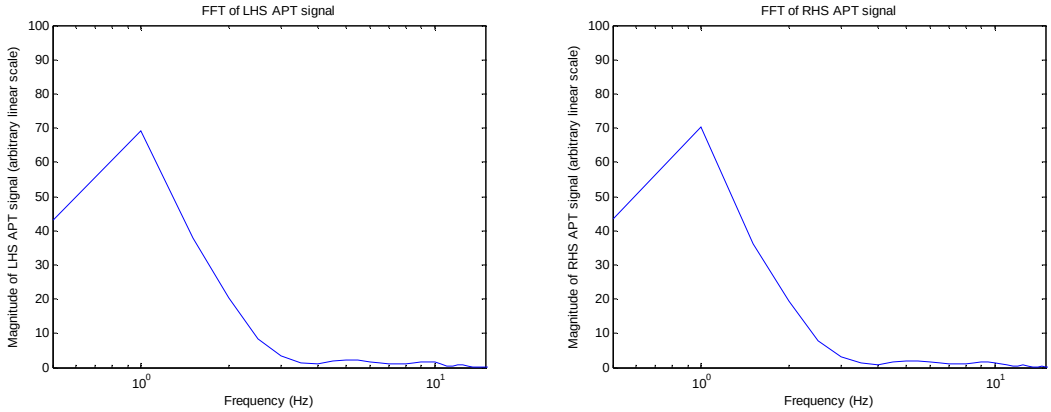

Figure 20: FFT of bus drive axle APTs – VSB 11-style step test as impulse. Test 251

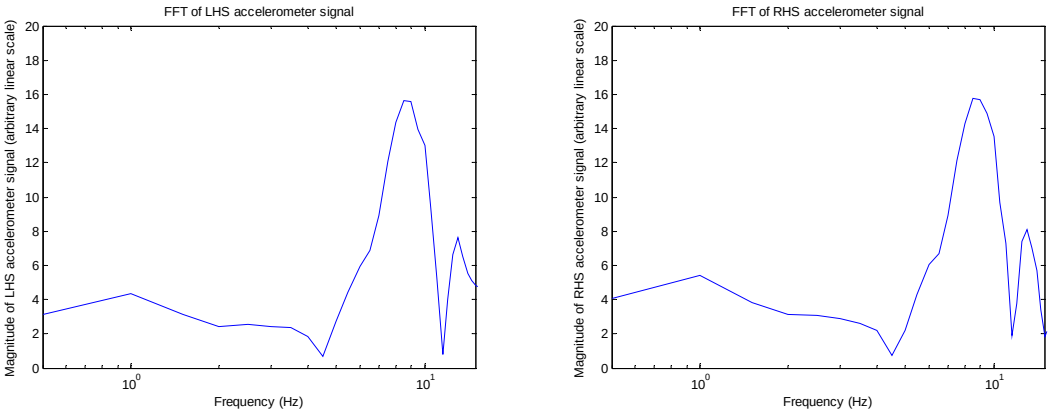

Figure 21: FFT of bus drive axle accelerometers – VSB 11-style step test as impulse. Test 251

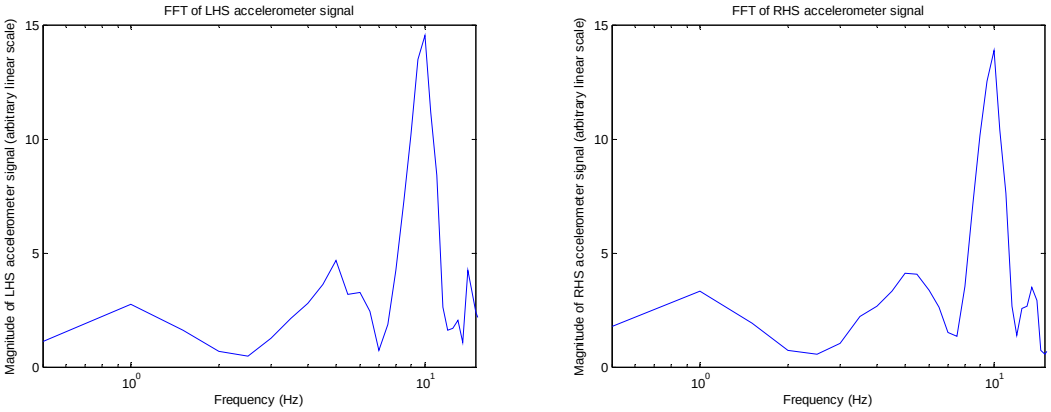

Figure 22: FFT of bus drive axle accelerometers – pipe test as impulse. Test 244

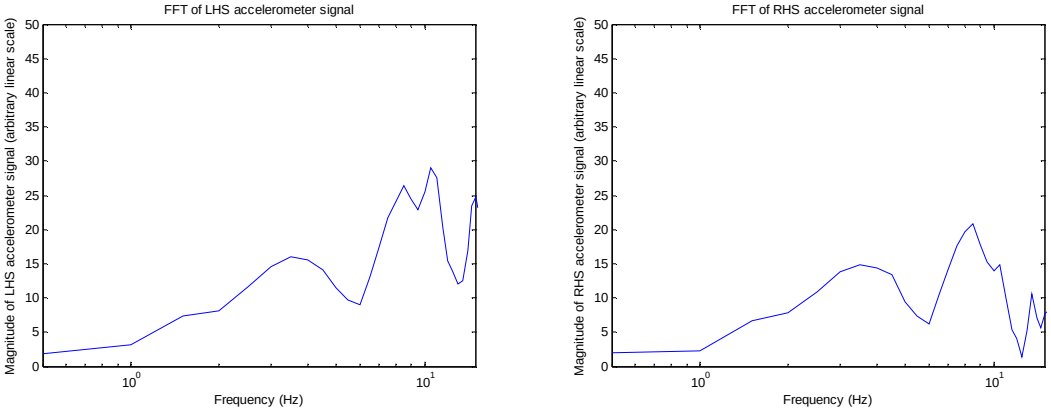

Figure 23: FFT of bus drive axle accelerometers – pipe test as impulse. Test 249

References

Australia Department of Transport and Regional Services. (2004). *Certification of road-friendly suspension systems; Road-friendly suspension certification requirements*. Canberra, ACT, Australia: Australia. Department of Transport and Regional Services.

Cebon, D. (Ed.). (1999). *Handbook of vehicle-road interaction*. Lisse, South Holland, Netherlands: Swets & Zeitlinger.

Chesmond, C. J. (1982). *Control system technology* (2nd ed.). Caulfield, Victoria, Australia: Edward Arnold.

Cole, D. J., & Cebon, D. (2007). Truck tyres, suspension design to minimise road damage. Retrieved 26 Oct 2007, from http://www-mech.eng.cam.ac.uk/trg/publications/downloads/veh_road/veh_road17.pdf

Costanzi, M., & Cebon, D. (2005). *Simulation of damage evolution in a spray sealed road.* (Technical report No. CUED/C-MECH/TR.90). Sydney: Cambridge University Engineering Department, Roads and Traffic Authority NSW.

Costanzi, M., & Cebon, D. (2006). *Simulation of damage evolution in a spray sealed road*. Paper presented at the International Symposium on Heavy Vehicle Weights and Dimensions, 9th, 2006, State College, Pennsylvania, USA.

Davis, L. (2006a). Background material used in preparation for paper; "Further developments in dynamic testing of heavy vehicle suspensions".

Davis, L. (2006b). *Dynamic load sharing on air-sprung heavy vehicles: can suspensions be made friendlier by fitting larger air lines?* Paper presented at the Australasian Transport Research Forum (ATRF), 29th, 2006, Gold Coast, Queensland, Australia.

Davis, L. (2006c). *Heavy vehicle suspension testing: on-board mass measurement system accuracy & tamper-vulnerability.* Brisbane, Queensland, Australia: Queensland Department of Main Roads.

Davis, L. (2007). *Further developments in dynamic testing of heavy vehicle suspensions*. Paper presented at the Australasian Transport Research Forum (ATRF), 30th, 2007.

Davis, L. (2008). *Larger air lines in heavy vehicle suspensions – differences in wheel and air spring forces*. Paper presented at the Australasian Transport Research Forum (ATRF), 31st, 2008.

Davis, L., & Bunker, J. (2007). *Heavy Vehicle Suspensions – Testing and Analysis. A literature review*. Brisbane, Queensland: Queensland Department of Main Roads; Queensland University of Technology.

Davis, L., & Bunker, J. (2008). *Suspension testing of 3 heavy vehicles – methodology and preliminary frequency analysis*. Brisbane, Queensland: Queensland Department of Main Roads; Queensland University of Technology.

Davis, L., Bunker, J., & Karl, C. (2008). *Technical Feasibility Assessment of On-Board Mass-Monitoring (OBM) Devices: a) Accuracy and robustness b) Ancillary systems analysis. Pilot test plan*. Brisbane, Queensland, & Melbourne, Victoria; Australia: Queensland Department of Main Roads; Queensland University of Technology; Transport Certification Australia.

Davis, L., Kel, S., & Sack, R. (2007). *Further development of in-service suspension testing for heavy vehicles.* Paper presented at the Australasian Transport Research Forum (ATRF), 30th, 2007, ATRF.

Davis, L., & Sack, R. (2004). *Analysis of heavy vehicle suspension dynamics using an on-board mass measurement system.* Paper presented at the Australasian Transport Research Forum (ATRF), 27th, 2004, Adelaide, South Australia, Australia.

Davis, L., & Sack, R. (2006). *Determining heavy vehicle suspension dynamics using an on-board mass measurement system*. Paper presented at the ARRB Conference, 22nd, 2006, Canberra, ACT, Australia.

de Pont, J. J. (1994). *Transit New Zealand Research Report, No: 29*. Wellington, New Zealand.

de Pont, J. J. (1999). Suspensions or whole vehicles? Rating road-friendliness. *International Journal of vehicle design, 6*(1-4), 23.

Doebelin, E. O. (1980). *System modelling and response - theoretical and experimental approaches*. New York, New York, USA: Wiley.

Duym, S., Stiens, R., & Reybrouck, K. (1997). Evaluation of shock absorber models *Vehicle System Dynamics, 27* 18.

European Council directive 85/3/EEC as amended by Council directive 92/7/EEC, (1996).

Fletcher, C., Prem, H., & Heywood, R. (2002). *Validation of dynamic load models.* (Technical documentation No. AP-T12). Sydney: Austroads.

Germanchev, A., & Eady, P. (2008). *On-board mass management accuracy and robustness testing - contract report*. Melbourne, Australia: ARRB.

Houpis, C. H., & Lamont, G. B. (1985). *Digital control systems theory, hardware, software*. New York, New York, USA: McGraw-Hill.

Jacob, B., & Dolcemascolo, V. (1998). *Dynamic interaction between instrumented vehicles and pavements*. Paper presented at the International Symposium on Heavy Vehicle Weights and Dimensions, 5th, 1998, Maroochydore, Queensland, Australia.

Karagania, R. M. (1997). *Road roughness and infrastructure damage. Master of Engineering Thesis.* Queensland University of Technology, Brisbane, Queensland, Australia.

Karl, C. (2007). *Project Plan: Technical Feasibility Assessment of On-Board Mass-Monitoring (OBM) Devices*. Melbourne: Transport Certification Australia Major Projects Division.

Mack-Volvo. (2007a). private correspondence. In L. Davis (Ed.) (mass of axle and wheel components ed.). Albury: Volvo Australia.

Mack-Volvo. (2007b). private e-mail correspondence. In L. Davis (Ed.) (damping ratio and frequency data request and response ed.). Chullora: Volvo Australia.

Meriam, J. L., & Kraige, L. G. (1993). *Engineering mechanics Vol 2 - Dynamics*. New York, New York, USA: Wiley.

Prem, H. (2008). Background information on methods for evaluating the dynamic-wheel-loading performance of heavy commercial vehicle suspensions.

Prem, H., George, R., & McLean, J. (1998). *Methods for evaluating the dynamic-wheel-loading performance of heavy commercial vehicle suspensions*. Paper presented at the International Symposium on Heavy Vehicle Weights and Dimensions, 5th, 1998, Maroochydore, Queensland, Australia.

Prem, H., Ramsay, E., McLean, J., Pearson, R., Woodrooffe, J., & de Pont, J. J. (2001). *Definition of potential performance measures and initial standards - performance based standards.* (Discussion paper). Melbourne, Victoria, Australia: National Road Transport Commission/Austroads.

Technical Committee ISO/TC 22. (2000). *Road vehicles - heavy commercial vehicle combinations and articulated buses - lateral stability test methods*. Geneva, Switzerland: ISO.

Thomson, W. T., & Dahleh, M. D. (1998). *Theory of vibration with applications*. Upper Saddle River, New Jersey: Prentice Hall.

Uffelmann, F., & Walter, W. D. (1994). *Protecting roads by reducing the dynamic wheel loads of trucks.* Paper presented at the 1994 European ADAMS conference ADAMS user conference, Frankfurt, Germany.